International Journal of Sediment Research 37 (2022) 383–398

Contents lists available at ScienceDirect

International Journal of Sediment Research

journal homepage: www.elsevier.com/locate/ijsrc

Original Research

Predictability performance enhancement for suspended sediment in rivers: Inspection of newly developed hybrid adaptive neuro-fuzzy system model

Rana Muhammad Adnan [a], Zaher Mundher Yaseen [b, c], Salim Heddam [d], Shamsuddin Shahid [e], Aboalghasem Sadeghi-Niaraki [f, g], Ozgur Kisi [e, h, *]

[a] State Key Laboratory of Hydrology-Water Resources and Hydraulic Engineering, Hohai University, Nanjing, 210098, China
[b] Department of Urban Planning, Engineering Networks and Systems, Institute of Architecture and Construction, South Ural State University, 76, Lenin Prospect, 454080 Chelyabinsk, Russia
[c] New Era and Development in Civil Engineering Research Group, Scientific Research Center, Al-Ayen University, Thi-Qar, 64001, Iraq
[d] Faculty of Science, Agronomy Department, Hydraulics Division University, 20 Août 1955, Route El Hadaik, BP 26, Skikda, Algeria
[e] School of Civil Engineering, Faculty of Engineering, Universiti Teknologi Malaysia (UTM), Johor Bahru, 81310, Malaysia
[f] Geoinformation Tech. Center of Excellence, Faculty of Geomatics Engineering, K.N.Toosi University of Technology, Tehran, Iran
[g] Department of Computer Science and Engineering, Sejong University, Seoul, Republic of Korea
[h] Civil Engineering Department, Ilia State University, Tbilisi, Georgia, USA

ARTICLE INFO

Article history:
Received 25 March 2021
Received in revised form
14 October 2021
Accepted 18 October 2021
Available online 24 October 2021

Keywords:
Suspended sediment load
Adaptive neuro-fuzzy system
Particle swarm optimization
Gravitational search algorithm

ABSTRACT

Reliable modeling of river sediments transport is important as it is a defining factor of the economic viability of dams, the durability of hydroelectric-equipment, river susceptibility to pollution, suitability for navigation, and potential for aesthetics and fish habitat. The capability of a new machine learning model, fuzzy c-means based neuro-fuzzy system calibrated using the hybrid particle swarm optimization-gravitational search algorithm (ANFIS-FCM-PSOGSA) in improving the estimation accuracy of river suspended sediment loads (SSLs) is investigated in the current study. The outcomes of the proposed method were compared with those obtained using the fuzzy c-means based neuro-fuzzy system calibrated using particle swarm optimization (ANFIS-FCM-PSO), ANFIS-FCM, and sediment rating curve (SRC) models. Various input combinations involving lagged river flow (Q) and suspended sediment (S) values were used for model development. The effect of Q and S on the model's accuracy also was assessed by including the difference between lagged Q and S values as inputs. The model performance was assessed using the root mean square error (RMSE), mean absolute error (MAE), Nash–Sutcliffe Efficiency (NSE), and coefficient of determination (R^2) and several graphical comparison methods. The results showed that the proposed model enhanced the prediction performance of the ANFIS-FCM-PSO (or ANFIS-FCM) models by 8.14% (1.72%), 14.7% (5.71%), 12.5% (2.27%), and 25.6% (1.86%), in terms of the RMSE, MAE, NSE and R^2, respectively. The current study established the potential of the proposed ANFIS-FCM-PSOGSA model for simulation of the cumulative sediment load. The modeling results revealed the potential effects of the river flow lags on the sediment transport quantification.

1. Introduction

River sedimentation affects most water engineering projects directly and significantly by reducing reservoir capacity, blocking dam inlets, and reducing channel capacity (Buyukyildiz & Kumcu, 2017; Calsamiglia et al., 2018). The river sedimentation also affects river water quality by reducing the dissolved oxygen concentration (Olyaie et al., 2015; Shiau & Chen, 2015). The effects of sedimentation on the hydro-environment have made it an important process in hydrology to be determined and accurately quantified. The major causes of sedimentation are weathering and erosion (Misset et al., 2019). However, the particle size and flow condition are the factors that most influence the sediment transportation (Zounemat-Kermani et al., 2020a). As erosion is the major cause of sedimentation, river sedimentation also is significantly influenced by various geomorphological, geological, and

* Corresponding author. Civil Engineering Department, Ilia State University, Tbilisi, 0162, Georgia.
E-mail address: ozgur.kisi@iliauni.edu.ge (O. Kisi).

https://doi.org/10.1016/j.ijsrc.2021.10.001
1001-6279/

meteorological factors (Chang et al., 2019). Generally, suspended sediment load (SSL) is estimated for the characterization of sediment in fluvial systems. Therefore, SSL is generally predicted to understand the possible changes in river sedimentation and management of hydraulic structures and river water quality.

The influence of multiple hydro-climatic and geomorphological factors on SSL and their complex interactions have made SSL modeling a tedious task (Samantaray & Ghose, 2018). Previous studies revealed that the pattern of SSL is highly complicated due to the influence of various hydro-climatic and geomorphological factors, including precipitation intensity, river discharge, and river bed sediment texture (Himanshu et al., 2017; Zounemat-Kermani et al., 2020b; Özger & Kabataş, 2015). This discussion indicates both nonlinear and non-stationarity attributes characterize SSL.

Various experimental and mathematical models are conventionally applied for modeling of SSL. The major drawback of experimental methods is their high cost. Further, experimental studies involve several assumptions for physical modelling of river flow, which add uncertainty in various model parameters, and thus, uncertainty in SSL estimation is increased (Aytek & Kişi, 2008; Ebtehaj et al., 2020; Shamaei & Kaedi, 2016). One of the most popular empirical methods of sediment calculation is the sediment rating curve (SRC) (Sharafati et al., 2020b; Tao et al., 2019). The empirical formulation of the SRC, based on river discharge is SSL $= aQ^b$, where Q is the river flow, and a and b are the rating curve parameters, respectively. Mathematical models also are widely employed for numerical simulation of SSL (Cao & Carling, 2003; Mohammadian et al., 2004). Conceptually, mathematical models are developed based on physical laws of fluvial sediment transportation. Numerous hydro-climatic and geomorphological parameters are required for developing SSL numerical models.These paramers are often not known. This makes the estimation accuracy of numerical models generally very low. In recent years, several empirical and data-driven models have been proposed to address the nonlinearity and complexity associated with SSL estimation. The literature suggests the higher capability of data-driven models compared to experimental and mathematical models in terms of estimation accuracy of SSL (Khan et al., 2019; Khosravi et al., 2018; Samantaray & Ghose, 2018).

Data-driven models based on artificial intelligence (AI) algorithms have been the choice for solving various engineering problems over the past decades (Fu, 2011; Hebert et al., 2014; Kleist, 2015; Sakurai et al., 2015). Various hydro-climatological phenomena have been successfully modeled using AI algorithms (Choubin et al., 2018b; Goyal & Ojha, 2011; Hoang & Bui, 2018; Samadi et al., 2014). Several review studies also reported the successful use of AI algorithms in SSL simulation (Gupta et al., 2021; Rajaee & Jafari, 2020; Rezaei et al., 2021). These studies revealed AI as the best alternatives for SSL estimation due to its simplicity and lower dependence on prior knowledge to address specific issues and accuracy in estimation (Salih et al., 2020). Furthermore, the convergence time of AI-based SSL estimation models is considerably lower than that for mathematical models. AI models can establish the patterns and variations in time-series datasets and efficiently replicate the physical processes. However, the previous studies have revealed the challenge in selecting the most appropriate data-driven algorithm in developing the SSL estimation model (Talebi et al., 2017).

Aytek and Kişi (2008) used genetic programming (GP), artificial neural network (ANN), and adaptive neuro-fuzzy inference system (ANFIS) in SSL estimation and showed the better skill of GP. Lafdani et al. (2013) evaluated the performance of ANN and support vector machine (SVM) in estimating SSL from rainfall and streamflow data and found ANN to outperform the SVMin. Tayfur et al. (2013) showed that a hybridized ANN-GA model performs better than the standalone ANN model in SSL estimation. Nourani and Andalib (2015) assessed the least squares support vector machine (LSSVM) and ANN models' performance in estimation SSL and found better performance using the ANN model.

Talebi et al. (2017) used regression trees and model trees for SSL estimation and reported better performance of the employed models than an ANN model. Choubin et al. (2018a) reported a better estimation of SSL using a classification and regression tree (CART) model from hydro-meteorological data than other AI models. The study also found the CART model was a good SSL estimation method in basins with limited hydro-meteorological data. Emamgholizadeh and Demneh (2019) studied the feasibility of GP, ANN, and ANFIS models in estimation of SSL and showed the better capability of GP. Adnan et al. (2019) predicted SSL using three different soft computing models namely, dynamic evolving neural fuzzy inference system (DENFIS), adaptive neuro-fuzzy inference system coupled with fuzzy c-means (ANFIS-FCM), and multivariate adaptive regression splines (MARS) models. They showed that the evolutionary fuzzy model DENFIS is more capable of simulating SSL than the other models. Khan et al. (2019) developed SSC estimation models using ANN and showed the possibility of using the model for accurate SSC estimation.

The advanced version of AI models has recently been used to improve the river's SSL predictability. For example, Ehteram et al. (2019) developed four hybrid AI models: adaptive neuro fuzzy system and bat algorithm (ANFIS-BA), adaptive neuro fuzzy system with weed algorithm (ANFIS-WA), multilayer feed-forward neural network with bat algorithm (MFNN-BA), and multilayer feed-forward neural network with weed algorithm (MFNN-WA) for the estimation of SSL in the Atrek River basin in Iran. They showed the better skill of ANFIS-BA compared to the other models. Salih et al. (2019) studied the properties of various advanced AI models, M5 model tree (M5P), attribute selected classifier (AS M5P), M5Rule (M5R), and K Star (KS), in estimating SSL at the Trenton meteorological station in the USA and reported the best performance using M5P. Banadkooki et al. (2020) employed the ANN-ant lion optimization (ALO), ANN-bat algorithm (BA), and ANN-particle swarm optimization (PSO) models in SSL estimation of a river in Iran and reported the higher potential of ANN-ALO in development of an SSL estimation model.

Recent studies have established that the hybridization of the standalone AI models using advanced metaheuristics algorithms can remarkably improve model efficiency. Over the past couple of years, this has also been observed in simulating many other hydrological processes, such as streamflow (Yuan et al., 2018), rainfall runoff (Adnan et al., 2021a), evaporation (Khosravi et al., 2019), evapotranspiration (Alizamir et al., 2020), solar radiation (Hou et al., 2018), hydraulics performance (Adnan et al., 2021b), water availability (Kaur et al., 2021), and several others. However, limited explorations have been done to assess the potential of hybrid models in simulating SSL. Hence, the efforts for exploring new advanced AI models in simulating sediment transport are still ongoing. In the current study, the feasibility of binary metaheuristic optimization algorithms including PSO and gravitational search algorithm (GSA) have been evaluated for tuning the parameters of fuzzy c-means based neuro-fuzzy systems in simulating river sediment load. The potential of the model was investigated through skill assessment of the models in simulating SSL using different statistical indices and graphical comparison methods.

2. Materials and methods

2.1. Case study

The Sacramento River basin was selected as the case study area to assess the proposed hybrid AI model (Fig. 1). The selected basin is the largest and longest river basin of California and has a key role by providing the 84% of the freshwater supply in California. The basin drains a catchment area of about 6,900 km^2. The yearly average precipitation in the basin is 914 mm, and the annual runoff of 27,600 m^3. The precipitation in the basin mainly occurs from November to March. The basin was selected as it is the main contributor of sediment to San Francisco Bay (produces 7 times higher sediment load than the San Joaquin River and accounts for almost 80% of the total sediment deposited to the San Francisco Bay-Delta). Accurate estimation of SSL is important for the wetland stability and ecology of the Bay-Delta.

Daily river flow and SSL data for the Sacramento River at Freeport gauging station (USGS Code No: 11447650) for the period of 1966–2015 were downloaded from the webserver of the USGS (http://co.water.usgs.gov/sediment/). The geographical location of the gauging station in the basin is 38°27′22N″ latitude and 121°30′01W″ longitude. The gauging station is about 21 km downstream from the confluence of American River within Sacramento. The data for the period 1966–2005 was used for training, and the remainder (2006–2015) were used for model testing.

Table 1 lists a brief statistical description of the data used in the current study. The table shows that both streamflow and sediment data are highly skewed (skewness ranges from 6.42 to 13.56).

2.2. Adaptive neuro-fuzzy inference system (ANFIS)

The adaptive neuro-fuzzy inference system (ANFIS) (Jang, 1993) is a robust hybrid, data-driven model. It can efficiently map the complex input-output relation for solving complex problems. ANFIS is designed as a hybrid model because it combines two properties: structured in several layers similar to ANN and using an inference engine based on the Takagi-Sugeno-Kang (TSK) fuzzy inference system (FIS) from fuzzy logic (Enayatollahi et al., 2020), based on a series of if-then rules and membership functions (MFs)

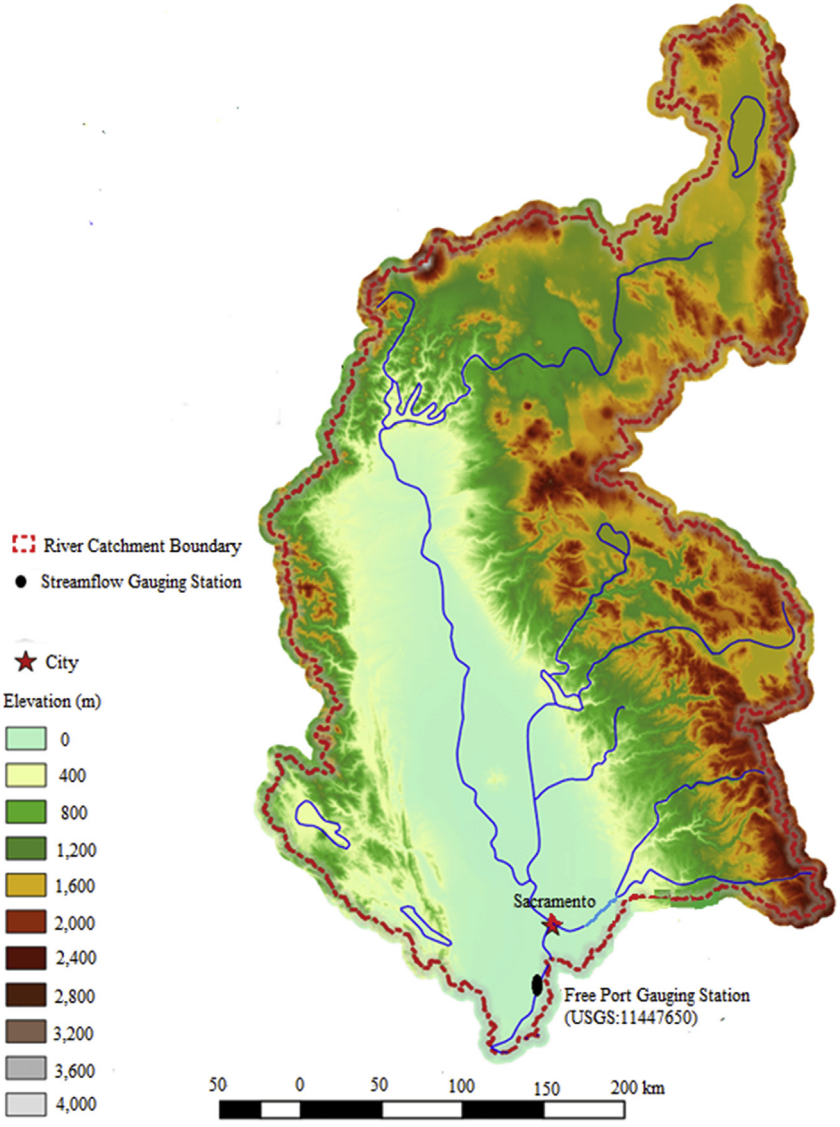

Fig. 1. Location map of the Sacramento River Basin.

Table 1
Statistical parameters of the Sacramento River data used in the current study.

	All data	Training	Test
	Streamflow (m^3/s)		
Mean	15.59	15.00	17.36
Min	0.016	0.016	0.055
Max	800	790	800
Median	4.96	4.75	5.48
Skewness	9.45	8.20	10.47
Std. dev.	40.9	37.6	49.7
	Sediment load (t/d)		
Mean	412	409	422
Min	0.002	0.002	0.055
Max	49,770	49,770	15,390
Median	40.80	35.83	57.85
Skewness	13.56	13.55	6.42
Std. dev.	1803	1,962	1,213

Note: Min = minimum, Max = maximum, Std. dev. = standard deviation.

(Soroush et al., 2019). Like other AI models, ANFIS contains two parameters (Fig. 2): linear and nonlinear. Linear parameters (fifth layer, Fig. 3), also called consequent parameters (p_i, q_i, and r_i) are optimized by the standard least squares method (LSM), while the nonlinear parameters (c_i and σ_i) are tuned using a backpropagation algorithm based on the principle of gradient descent (second layer, Fig. 3).

During the training process, all linear and nonlinear parameters are optimized simultaneously to determine the best relationships among all possible fuzzy rules (Kisi et al., 2018). In ANFIS, the fuzzy rules are created using the FIS. The fuzzification and defuzzification are the most critical steps of ANFIS model development (Muhammad Adnan et al., 2019). For simplicity, an ANFIS architecture utilized was consisting of only two inputs (x_1, x_2), one output (f) and three fuzzy sets for each input (A_1, A_2, A_3, and B_1, B_2, B_3, respectively) as indicated in Fig. 3. The proposed ANFIS model consists of six layers: the input layer, fuzzification layer, the rules (e.g., product) layer, the normalization layer, the defuzzification layer, and the total output (e.g., summation) layer. Among them, two are adaptive layers, and three are fixed layers (Adedeji et al., 2020). The if-then rules for developing a fuzzy model can be expressed as follows (Sharafati et al., 2020c):

$$\text{Rule1} = \text{If}\,(x_1\,\text{is}\,A_1)\,\text{and}\,(x_2\,\text{is}\,B_1)\,\text{Then}\,(f_1 = p_1x_1 + q_1x_2 + r_1) \quad (1)$$

$$\text{Rule2} = \text{If}\,(x_1\,\text{is}\,A_2)\,\text{and}\,(x_2\,\text{is}\,B_2)\,\text{Then}\,(f_2 = p_2x_1 + q_2x_2 + r_2) \quad (2)$$

$$\text{Rule3} = \text{If}\,(x_1\,\text{is}\,A_3)\,\text{and}\,(x_2\,\text{is}\,B_3)\,\text{Then}\,(f_3 = p_3x_1 + q_3x_2 + r_3) \quad (3)$$

where x_1 and x_2 are the input variables, A_i and B_i are the fuzzy sets, {p_i, q_i, and r_i} are the linear or consequent parameters of the fuzzy rules, and f is the output variable. The layers are described as follows:

Layer 1. This is a layer without any mathematical operator. ANFIS takes the input variables (x_i) through this layer.

Layer 2. This is the fuzzification layer, in which every node, i is an adaptive node with a node function. This layer maps x_i to the fuzzy sets A_i and B_i and decides the membership degree of the corresponding fuzzy set (Jiang et al., 2020). This layer contains the premise (nonlinear) parameters, which correspond to the parameters of the membership function.

Layer 3. This is the layer of rules. This layer's neurons are labelled by Π, which are fixed nodes and only act as a simple multiplier. In practice, the equivalent of if-then part and the "AND" rule are used to identify the corresponding firing power (Adıgüzel et al., 2019).

Layer 4. This is known as the normalization layer, which consists of neurons labelled by N. These are fixed nodes used for estimating the normalized firing strength. The nodes calculate the part of the contribution of the rule (Adıgüzel et al., 2019).

Layer 5. This is the defuzzification layer which is also called the aggregation layer. These nodes are adaptive whose output is the product of normalized firing strength (Adıgüzel et al., 2019).

Layer 6. This is a single node layer used to deliver the model output. This node sums up all the signals to estimate the output.

An ANFIS model is trained to determine the best linear (p_i, q_i, and r_i) and nonlinear (c_i and σ_i) parameters. The training algorithm often is hybridized or combined simultaneously with the back-propagation algorithm using gradient descent for optimizing the linear (consequent) parameters and the least squares method (LSM) for optimizing the nonlinear (premise) parameters. However, the critical step in training an ANFIS model is to find the optimum number of fuzzy rules. Three methods are widely used for determining the number of fuzzy rules: (i) ANFIS with the gird partition method called ANFIS_G, (ii) ANFIS with the subtractive clustering (SC) called ANFIS_S, and (iii) ANFIS with fuzzy c-means clustering (FCM) called ANFIS_FCM. It has been found that two clustering methods (SC and FCM) are more suitable to avoid the so-called "*curse of dimensionality*" encountered due to the use of the gird partition method and the necessity of generating fewer fuzzy rules (Zare & Koch, 2018). In current study, the FCM clustering technique was applied for determining the number of fuzzy rules. For this purpose, a cluster number was specified, and the correspondence of each cluster to one fuzzy rule was determined. It has been demonstrated that the FCM possess has several advantages, including high speed, use of less rules, and higher accuracy (Naderpour & Mirrashid, 2020).

2.3. Hybrid ANFIS models and metaheuristic optimization methods

During the optimization of the ANFIS parameters using the backpropagation training algorithm, the convergence towards a local minimum instead of the global minima is the most widely encountered problem. One of the most and promising solutions proposed in recent years to avoid trapping at local minima is the use of the metaheuristic bioinspired methods, such as GSA, PSO, firefly optimization algorithm (FFA), genetic algorithm (GA), grey wolf optimizer (GWO), and the biogeography-based optimization (BBO) among others. The metaheuristic methods transform the problem into an optimization task to evade the localized trapping (Enayatollahi et al., 2020). In this study, two algorithms, PSO and GSA, were used to optimize ANFIS parameters. The hybrid models were named ANFIS-FCM-PSO and ANFIS-FCM-PSOGSA, respectively. Figure 2 shows the complete flowchart of the proposed models. The models are described in the following subsections.

2.4. ANFIS-FCM-PSO

PSO (Eberhart & Kennedy, 1995) is a metaheuristic bio-inspired swarm intelligence approach inspired by birds and fishes' biological and sociological behavior in finding food (Enayatollahi et al., 2020; Sharafati et al., 2020a). A population of particles called a swarm, which forms the search space, is used to find the best solution considering each one as a solution to the problem. An interaction between the particles in the population forms the neighborhood topology. The particles are derived from

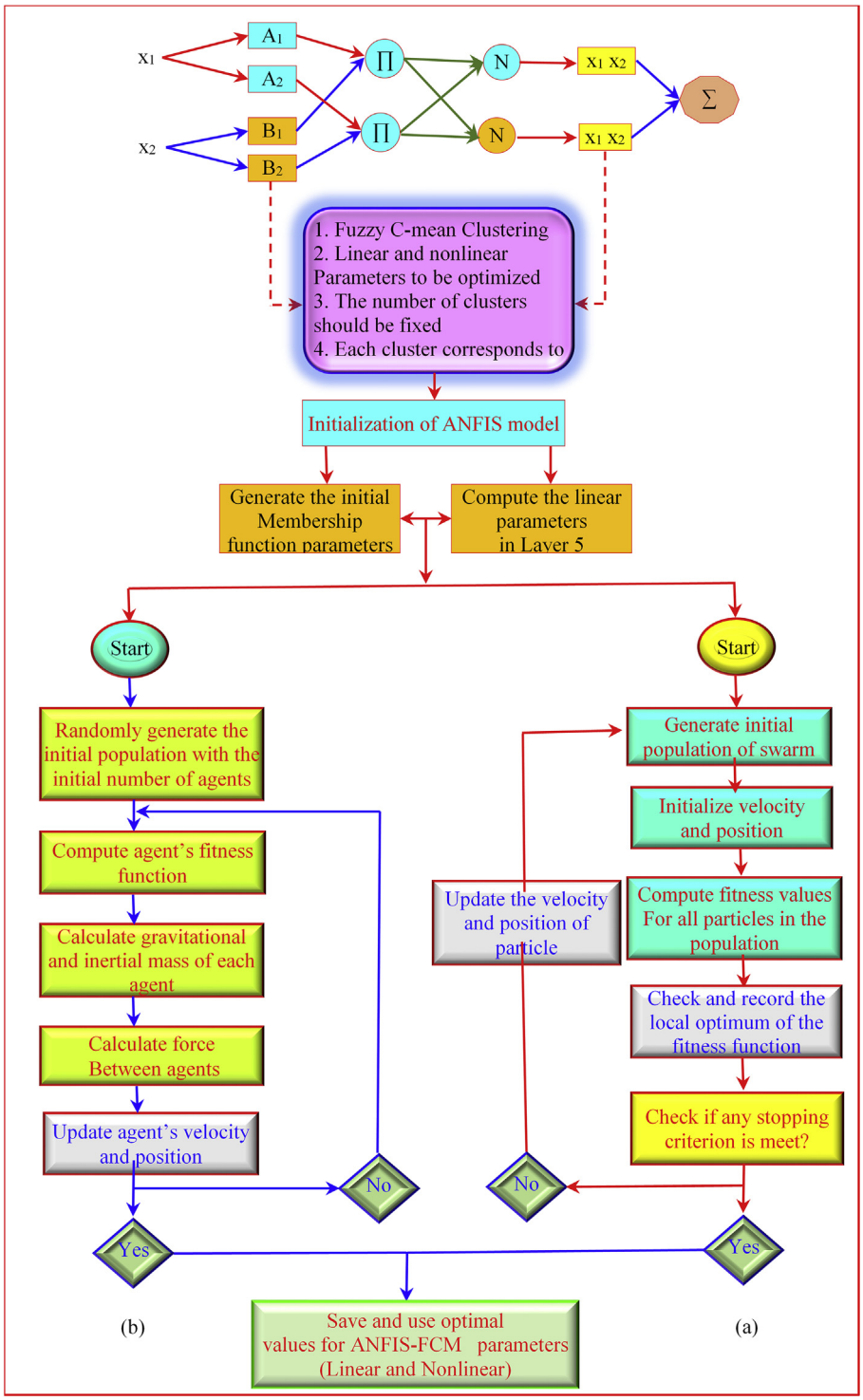

Fig. 2. Flowchart of the proposed models: (a) ANFIS-FCM-PSO and (b) ANFIS-FCM-PSOGSA.

moving in the direction of a global solution. The velocities and positions of the particles were randomly initialized in a multi-dimensional search space in each iteration and, subsequently, the location and speed of particles. The location and velocity of each particle are updated using a fitness function in each iteration (Mosa, 2020). From a mathematical point of view, each particle has an individual best location (P_{best}) and a global best (G_{best}) location, which is calculated considering the position among all particles (Anemangely et al., 2017; Ray et al., 2021). Finally, the new position of each particle is decided, depending on its best previous location and the location of the best particle in the entire population (Zanganeh, 2020). The iterative process continues until both conditions are ultimately satisfied according to the defined fitness function. For a N dimensional optimization size, at each generation, k, the particles' velocity and location are updated as follows:

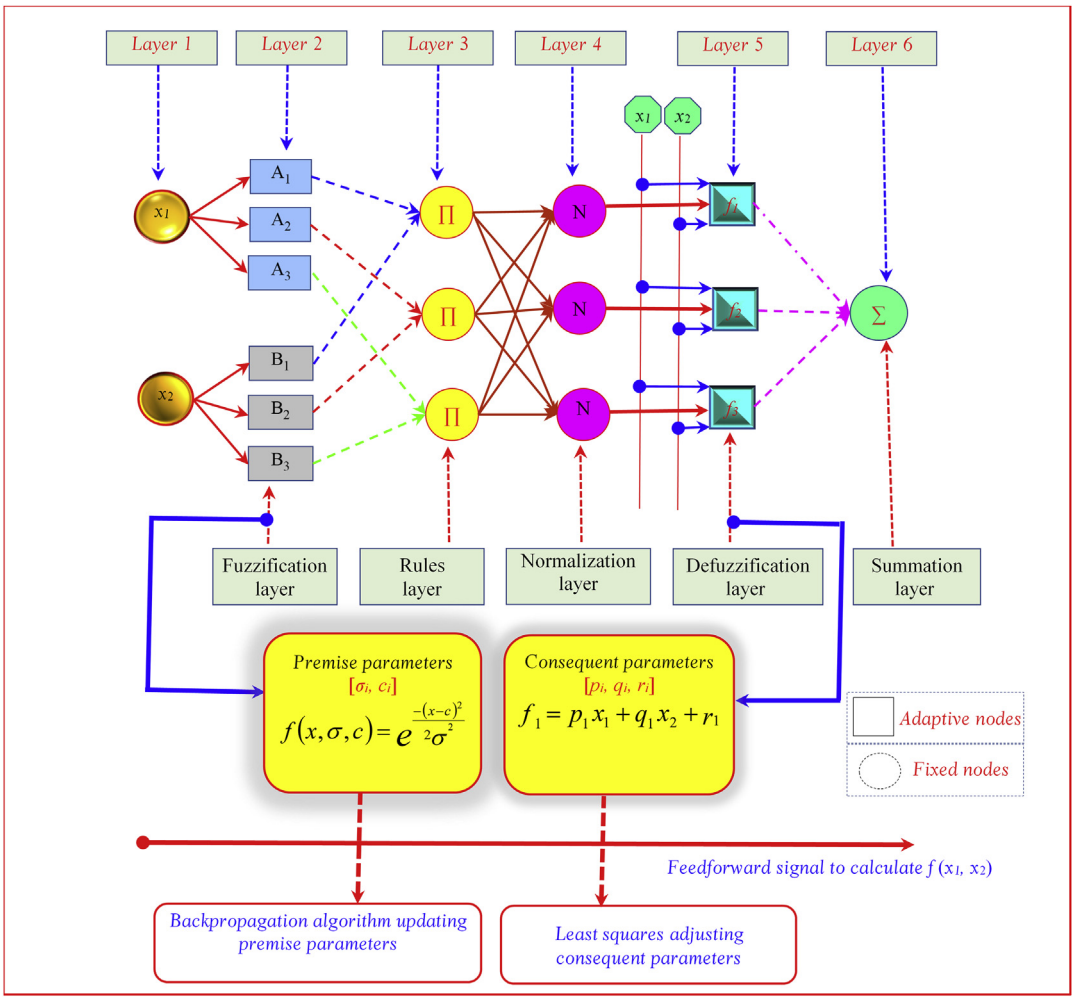

Fig. 3. Adaptive neuro-fuzzy inference system (ANFIS) with two input variables (x_1, x_2) and three fuzzy sets for each input variable.

$$v_{i,n}(t+1) = w * v_{i,n}(t) + C_1 r_1 \left(x^d_{\text{Pbest}_i} - x^d_i(t)\right) + C_2 r_2 \left(x^d_{\text{Gbest}_i} - x^d_i(t)\right) \quad (4)$$

$$x^d_i(t+1) = x^d_i(t) + v^d_i(t+1) \quad (5)$$

where the constants C_1 and C_2 are referred to as the acceleration constants, r_1 and r_2 are arbitrary values between 0 and 1, x_{Pbest} is the preceding best location of the i-th particle in generation k, x_{Gbest} is the preceeding global best location of the all particles in generation k, $x_i = (x_{i1}, x_{i2}, \ldots, x_{iD})$ represent the current position vector of the particle in a D-dimensional search space, $v_i = (v_{i1}, v_{i2}, \ldots, v_{iD})$ represent the velocity of the i-th particle, and w is known as the inertia weight (Eappen & Shankar, 2020; Mallick et al., 2013). PSO was used for the optimization of the ANFIS-FCM model's hyper-parameters. Figure 2a shows the flowchart of ANFIS-FCM-PSO model.

2.5. ANFIS-FCM-PSOGSA

GSA (Rashedi et al., 2018) uses the concept of Newton's gravitation law. GSA is a metaheuristic optimization approach that belongs to physics-based intelligent heuristic methods (Özkaraca, 2018). GSA has two major components: the agents and their corresponding masses. The agents responded to the force of gravity and also exerted a pull on one another. Thus, the final response to gravity is measured by their masses. Each object has four components: (i) position, (ii) inertial mass, (iii) passive mass, and (iv) active gravitational mass, and one solution governed by the gravitational and inertia masses (Dokeroglu et al., 2019). The best solution in the GSA algorithm corresponds to the heaviest agent, and consequently, all other agents are attracted and move towards the best solution. A fitness function is evaluated for each object in each iteration until the optimal solution, which is the final location of the agent having the highest inertial mass, is achieved (Jiang et al., 2020). GSA can be formulated as follows. For N search masses (i.e., agents) in a search space with n dimensions, the position of the i-th solution (i.e., mass) can be expressed as vector X_i as follows (Faris et al., 2018):

$$X_i = \left(x^1_i, x^2_i, \ldots, x^d_i, \ldots x^n_i\right), i = 1, 2, \ldots, N \quad (6)$$

where x^d_i is the position of i-th mass in d-th dimension, and n is the dimension of the search space. At a specific time t, the gravitational (m_i) and inertial (M_i) masses for the i-th agent is linked to the fitness function of that agent and updated as follows (Naganna et al., 2019):

$$m_i(t) = \frac{fit_i(t) - worst(t)}{best(t) - worst(t)} \tag{7}$$

$$M_i(t) = \frac{m_i(t)}{\sum_{j=1}^{N} m_j(t)} \tag{8}$$

where $fit_i(t)$ is the cost function (fitness) of the particle (i.e., agent i), $best(t)$ and $worst(t)$ correspond to the best and worst of the objective function among all agents at time t, respectively, and $M_i(t)$ is the inertial mass of agent i. Consequently, during the training process, the agents change their location at each iteration. The velocity and location of the agents at the proceeding step are modified as follow (Faris et al., 2018):

$$v_i^d(t+1) = \beta_i v_i^d(t) + a_i^d(t) \tag{9}$$

$$x_i^d(t+1) = x_i^d(t) + v_i^d(t+1) \tag{10}$$

where β is a random number ($0 \le \beta \le 1$), x is the position of the agent, a_i is the acceleration of the i-th agent at the current iteration, and t is calculated as follows (Faris et al., 2018):

$$a_i^d(t) = \frac{F_i^d(t)}{M_i(t)} \tag{11}$$

where M_i is the mass of object i, and $F_i^d(t)$ is the total gravitational force acting on the i-th agent from agent j at the d-th dimension and i-th iteration, and it can be calculated between two particles (i.e., agents) i and j as follows (Mirjalili et al., 2012):

$$F_{ij}(t) = G(t)\frac{M_i(t) \times M_j(t)}{R^2} \times \left[x_j(t) - x_i(t)\right] \tag{12}$$

where G is the gravitational constant and R is the distance between particle j and particle i. Here x_i and x_j are the position vector of the i-th and jth agents in the d-th dimension.

Recently, a new hybrid algorithm, composed of PSO and GSA, has been developed to take advantage of the two paradigms (i.e., PSO and GSA). The idea behind the development of the PSOGSA is to enhance the searching ability of G_{best} in PSO and the local search capability of the GSA. Several authors have highlighted the advantages and the benefits of combining the two paradigms: (i) the high abilities of GSA in "*exploitation*" and PSO in "*exploration*" aspects (Bounar et al., 2019), (ii) GSA is excellent in local search while PSO make the most rapid contribution for achieving the goal of an optimum value very quickly (Eappen & Shankar, 2020), (iii) balancing the "*global searching*" and "*local searching*" is of importance (Mirjalili et al., 2012), and (iv) each particle in the population of the hybrid PSOGSA uses the PSO velocity and GSA acceleration to update its position (Jiang et al., 2014). From a mathematical point of view, the position "x" and the velocity "v"of any agent is calculated as follows (Meshram et al., 2019a, 2019b):

$$v_i(t+1) = w \times v_i(t) + c_1' \times r_1 \times ac_i(t) + c_2' \times r_2 \times (G_{best} - X_i(t)) \tag{13}$$

$$X_i(t+1) = X_i(t) + v_i(t+1) \tag{14}$$

where $v_i(t)$ is the velocity of agent i at iteration t; w the inertia weight; r_1 and r_2 are random numbers; $ac_i(t)$ is the acceleration of agent i at iteration t, c_1' and c_2' are the acceleration coefficients used for adjusting the influence of PSO velocity and GSA acceleration, respectively, and G_{best} is the optimal solution (Meshram et al., 2019a, 2019b; Sharafati et al., 2020a).

The current study used PSOGSA to optimize the linear (premise) and nonlinear (consequent) parameters of the ANFIS-FCM model. The mean squared error (MSE) was used as the fitness function. The flowchart of ANFIS-FCM-PSOGSA model is presented in Fig. 2b.

2.6. Data preparation and model scenarios

Ten different input combinations consisting of lagged values of river flow and SSL and their variability with time were used to develop the SSL estimation models and quantify the variables' influence on the SSL. Different input combinations utilized in this study are listed in Table 2. The first four models were developed using different combinations of the present and three antecedent values of river flow (Q_t, $Q_{t\text{-}1}$, $Q_{t\text{-}2}$, $Q_{t\text{-}3}$) as inputs. Therefore, the inputs for the first four models were river discharges, as listed in Table 2. More lagged Q inputs beyond three steps (e.g., $Q_{t\text{-}3}$) did not improve the model accuracy. Next, three lagged values of SSL (S_t to $S_{t\text{-}1}$, $S_{t\text{-}2}$, $S_{t\text{-}3}$) were added as inputs. Therefore, models 5 to 7 were developed using lagged SSL values (Table 2). The Best Q (Best S) in Table 2 indicates the best input combination of $Q(S)$, which provides the best accuracy in the testing period. The Best Q or Best S combination can change for each method. Therefore these combinations could not be written in respect of Q and S variables.

The effect of variation of Q and S with time was also considered as inputs. Input combination 8 was the best Q, the best S, and river flow difference between two periods, Q_t–$Q_{t\text{-}1}$. Similarly, the variation of SSL between two periods, $S_{t\text{-}1}$–$S_{t\text{-}2}$ was considered the input for combination 9. The combined effect of the best Q, the best S, and the variations of both inputs were considered in input combination 10. After selecting the 10 input combinations for the three selected algorithms, normalization of input and output data was done to scale the data in the range of 0–1 using the following equation:

$$(Q/S)_n = \frac{(Q/S)_a - \min(Q/S)}{\max(Q/S) - \min(Q/S)} \tag{15}$$

where $(Q/S)_n$ and $(Q/S)_a$ are the normalized and actual Q or S data, respectively, and the $\min(Q/S)$ and $\max(Q/S)$ are the minimum and maximum values of Q or S dataset, respectively.

For the development of ANFIS-FCM models, different membership functions were evaluated for the different numbers of clusters. The major parameters selected for standalone ANFIS-FCM and hybrid ANFIS-FCM-PSO and ANFIS-FCM-PSOGSA models are enlisted in Table 3. The Gaussian membership function was finally utilized with cluster size ranges from 2 to 10. The effects of input combination on estimation accuracy were evaluated based on the performance of the standalone ANFIS-FCM model and both hybrid models. Swarm size for the PSO was selected as 100 because a greater number did not improve the model accuracy.

2.7. Evaluation metrics

The ability of the hybrid ANFIS-FCM-PSOGSA model in estimating daily SSL in comparison to hybrid ANFIS-FCM-PSO and standalone ANFIS-FCM models was evaluated using three statistical metrics which are defined as follows:

Table 2
Different input combinations used for the selection of optimal input combination for the estimation of sediment loads.

	Input combinations	Models		
		ANFIS-FCM	ANFIS-FCM-PSO	ANFIS-FCM-PSOGSA
1	Q_t	ANFIS-FCM1	ANFIS-FCM-PSO1	ANFIS-FCM-PSOGSA1
2	Q_{t-1} and Q_t	ANFIS-FCM2	ANFIS-FCM-PSO2	ANFIS-FCM-PSOGSA2
3	Q_{t-2}, Q_{t-1}, and Q_t	ANFIS-FCM3	ANFIS-FCM-PSO3	ANFIS-FCM-PSOGSA3
4	Q_{t-3}, Q_{t-2}, Q_{t-1}, and Q_t	ANFIS-FCM4	ANFIS-FCM-PSO4	ANFIS-FCM-PSOGSA4
5	Best Q and S_{t-1}	ANFIS-FCM5	ANFIS-FCM-PSO5	ANFIS-FCM-PSOGSA5
6	Best Q, S_{t-1}, and S_{t-2}	ANFIS-FCM6	ANFIS-FCM-PSO6	ANFIS-FCM-PSOGSA6
7	Best Q, S_{t-1}, S_{t-2}, and S_{t-3} Variation input included	ANFIS-FCM7	ANFIS-FCM-PSO7	ANFIS-FCM-PSOGSA7
8	Best Q, Best S, Q_t–Q_{t-1}	ANFIS-FCM8	ANFIS-FCM-PSO8	ANFIS-FCM-PSOGSA8
9	Best Q, Best S, S_{t-1}–S_{t-2}	ANFIS-FCM9	ANFIS-FCM-PSO9	ANFIS-FCM-PSOGSA9
10	Best Q, Best S, Q_t–Q_{t-1}, S_{t-1}–S_{t-2}	ANFIS-FCM10	ANFIS-FCM-PSO10	ANFIS-FCM-PSOGSA10

Best *Q* (Best *S*) indicates the best input combination of *Q*(*S*) which provides the best accuracy for the testing period.

$$\text{Mean absolute error (MAE)} = \frac{1}{N}\sum_{i=1}^{N}\left|(S_0)_i - (S_C)_i\right| \tag{16}$$

$$\text{Root mean square error (RMSE)} = \sqrt{\frac{1}{N}\sum_{i=1}^{N}\left[(S_0)_i - (S_C)_i\right]^2} \tag{17}$$

$$\text{Nash–Sutcliffe Efficiency (NSE) (Nash \& Sutcliffe, 1970)} = 1 - \frac{\sum_{i=1}^{N}\left[(S_0)_i - (S_C)_i\right]^2}{\sum_{i=1}^{N}\left[(S_0)_i - \overline{S}_0\right]^2} \tag{18}$$

$$\text{Coefficient of Determination } \left(R^2\right) = \frac{\sum_{i=1}^{N}\left[\left((S_0)_i - (\overline{S_0})\right)\left((S_C)_i - (\overline{S_C})\right)\right]}{\sum_{i=1}^{N}\left[(S_c)_i - (\overline{S_c})\right]^2\sum_{i=1}^{N}\left[(S_0)_i - (\overline{S_0})\right]^2} \tag{19}$$

where N is the data number; S_o, S_c, $\overline{S}_0$, and $\overline{S_c}$ are the observed, computed, mean of observed daily, and mean of computed daily SSL, respectively.

Table 3
Major parameters of ANFIS-FCM, ANFIS-FCM-PSO, and ANFIS-FCM-PSOGSA models optimized for improved estimation of sediment loads.

Model	Parameter	Description/ Value
ANFIS-FCM	Membership Function Type	Gaussian
	Output Membership Function Type	Linear
	Membership Function Range	2–10
	Inputs/Output	1–10/1
	Fuzzy Structure	Takagi-Sugeno
	Cluster Range	2–10
	Number of fuzzy rules	10
	Number of epochs	100
	Initial Step size	0.01
	Step size decrease rate/step size increase rate	0.9/1.1
ANFIS-FCM-PSO	Number of Iteration	1,000
	Cognitive acceleration (c1)	1
	Social acceleration (c1)	2
	Swarm size	100
ANFIS-FCM-PSOGSA	Number of Iteration	1,000
	Initial Gravitational constant	1
	Descending coefficient	20
	Swarm size	100

3. Results

The performance of the standalone ANFIS-FCM in estimating the SSL for 10 different input combinations during training and testing based on different statistical indicators are listed in Table 4. When only river flow was considered as the inputs (i.e., ANFIS-FCM1 to ANFIS-FCM4), the models showed low accuracy, with the mean values of RMSE, MAE, NSE, and R^2 of 4,429 t/d, 2,179 t/d, 0.145, and 0.538 in the testing phase, respectively. The best *Q*-based input combination for the ANFIS-FCM model for the testing phase was found for the first input combination (i.e., ANFIS-FCM1) consisting of only river flow at time t (Q_t) or the present river flow. The estimation accuracy was noticed to decrease gradually from ANFIS-FCM1 to ANFIS-FCM4. Compared to ANFIS-FCM4, ANFIS-FCM1 provided a 5.55% lower RMSE, 18.4% lower MAE, 43.9% higher NSE, and 4.6% higher R^2 in the testing phase. Next, the performance using the best SSL input combination in addition to the best *Q* input combination (ANFIS-FCM1) was evaluated. Table 4 shows a strong influence of the lagged SSL values on model estimation accuracy. Adding just one lagged value of SSL as input with Q_t (ANFIS-FCM5), the RMSE and MAE decreased 59.4% and 62.8%, and the NSE and R^2 increased 320% and 55.9%, respectively, compared to ANFIS-FCM1 in the testing phase.

For input combinations of 5–7, all ANFIS-FCM models (ANFIS-FCM5–ANFIS-FCM7) showed improvement in SSL estimation according to the mean RMSE, MAE, NSE and R^2 (1,640 t/d, 729.6 t/d, 0.883 and 0.890, respectively) in the testing phase. Therefore, the three lagged values of SSL (S_{t-1}, S_{t-2}, S_{t-3}) were selected as the best *S* input combination (ANFIS-FCM7) along with Q_t. The evaluation of the effect of the variation of *Q* and *S* with time on SSL estimation accuracy yielded no improvement in the estimation accuracy of ANFIS-FCM model in the testing phase (ANFIS-FCM8 and ANFIS-FCM9) (Table 4). Compared to the combination of the best *S* and best *Q* inputs (ANFIS-FCM7), ANFIS-FCM8 showed higher RMSE, 1,628 t/d (2.26%) and MAE, 785 t/d (7.97%) and lower NSE, 0.884 (0. 67%) and lower R^2, 0.893 (0.44%) in the testing phase. However, in comparison to the best *Q* input combination (ANFIS-FCM1), ANFIS-FCM8 showed an improvement in estimation accuracy with reduction in RMSE from 4,163 to 1,262 (60.9%), MAE from 1,940 to 785 (59.5) and increase in NSE and R^2 from 0.207 to 0.884 (327%), and from 0.561 to 0.893 (59.1%), respectively. The variation of sediment load as input could not be evaluated for standalone ANFIS-FCM models due to an error in simulation. The 10th input combination produced the same results as the 8th input combination.

Table 4
Results of the ANFIS-FCM in modeling suspended sediment load.

Input	Cluster number	Training			R^2	Test			R^2
		RMSE	MAE	NSE		RMSE	MAE	NSE	
ANFIS-FCM1	10	6,287	2,409	0.653	0.653	4,163	1,940	0.244	0.561
ANFIS-FCM2	6	5,958	2,349	0.688	0.688	4,329	1,966	0.183	0.523
ANFIS-FCM3	2	6,270	2,689	0.655	0.655	424	2,278	0.147	0.533
ANFIS-FCM4	2	6,146	2,696	0.668	0.669	4,503	2,337	0.116	0.536
ANFIS-FCM5	2	3,653	1,180	0.883	0.883	1,732	735	0.869	0.871
ANFIS-FCM6	2	3,280	1,078	0.906	0.906	1,596	727	0.889	0.892
ANFIS-FCM7	2	3,241	1,084	0.908	0.908	1,592	727	0.889	0.897
ANFIS-FCM8	2	2,855	1,006	0.928	0.928	1,628	785	0.884	0.893
ANFIS-FCM9	None	None	None	None	None	None	None	None	None
ANFIS-FCM10	2	2,855	1,006	0.928	0.928	1,628	785	0.884	0.893

Note: RMSE and MAE are in t/d.

Table 4 shows that most of the input combinations found 2 as the optimal number of clusters. However, ANFIS-FCM1 and ANFIS-FCM2 produced the best results for 10 and 6 clusters, respectively.

The estimation accuracies of the hybrid ANFIS-FCM-PSO models during training and testing are listed in Table 5**.** The results indicate that for the testing phase, only the river flow as input (Q_t) provided a more accurate estimation than its combination with antecedent river flow values. The ANFIS-FCM-PSO1 model's estimation accuracy was much higher than the ANFIS-FCM-PSO4 model. The RMSE of ANFIS-FCM-PSO1 model was 4.51% lower than that for the ANFIS-FCM-PSO4, MAE was less by 12.9% and NSE and R^2 were higher by 28.3% and 5.54% in the testing phase, respectively. Similar to the performance of ANFIS-FCM model, the inclusion of the lagged values of SSL as inputs with Q_t as input yielded a large improvement in estimation accuracy for the ANFIS-FCM-PSO models. The ANFIS-FCM-PSO7 (S_{t-1}, S_{t-2}, S_{t-3}, and Q_t) was found to be the best model with both the best S and Q combinations as input. ANFIS-FCM7 reduced the RMSE from 4,265 to 1,576 t/d (63.0%), MAE from 1,974 to 649 t/d (67.1%), and increased the NSE and R^2 from 0.207 to 0.892 (331%) and 0.567 to 0.900 (58.7%), respectively, compared to ANFIS-FCM-PSO1 (best model with Q_t as input) in the testing phase.

In contrast with the performance of the ANFIS-FCM model, the inclusion of variations in Q and S with time yielded an improvement in estimation accuracy of the ANFIS-FCM-PSO models with mean RMSE, MAE, NSE, and R^2 of 1,557 t/d, 627 t/d, 0.894 and 0.902 in the testing phase, respectively. ANFIS-FCM-PSO8 composed of best Q, best S, and variation of Q with time (Q_t–Q_{t-1}) as inputs provided more accuracy in estimation compared to ANFIS-FCM7 with a lower RMSE of 1,557 t/d (1.21%), MAE of 627 t/d (3.38), and higher NSE and R^2 of 0.894 (0.22%) and 0.902 (0.22%), respectively, in the testing phase. Tables 4 and 5 also show an improvement in the performance of the standalone ANFIS-FCM model when its parameters were optimized using the PSO optimization algorithm. Overall, ANFIS-FCM-PSO models were able to reduce the estimation error of the standalone ANFIS-FCM models by reducing the mean RMSE from 2,876 to 2,681 t/d (6.81%), mean MAE from 1,386 to 1,253 t/d (9.57%), and increasing the mean NSE from 0.554 to 0.610 (9.98%) and 0.731 to 0.752 (2.82%), respectively, in the testing phase. The hybrid models also indicated that the lagged values of SSL have key roles in the estimation of SSL.

The hybrid ANFIS-FCM-PSOGSA models' performance is summarized in Table 6. Like the other two models, ANFIS-FCM-PSOGSA1 model comprising only the present river flow as input (Q_t) showed higher performance in the testing phase than the models with other antecedent river flow values as input. ANFIS-FCM-PSOGSA1 reduced the RMSE and MAE compared to ANFIS-FCM-PSOGSA4 by 5.26% and 3.48%, respectively, and increased NSE and R^2 by 30.1% and 4.72%, respectively, in the testing phase. Similar to the other two modeling algorithms, the inclusion of lagged values of SSL along with Q_t as inputs increased the estimation accuracy with mean RMSE of 1603 t/d, MAE of 639 t/d, NSE of 0.888, and R^2 of 0.895. ANFIS-FCM-PSOGSA7 performed the best indicating S_{t-1}, S_{t-2}, S_{t-3}, and Q_t as the best input combination for estimating SSL. ANFIS-FCM-PSOGSA7 reduced the RMSE from 4,107 to 1,554 t/d (62.1%), MAE from 1,925 to 628 t/d (67.4%), and increased the NSE and R^2 from 0.265 to 0.895 (238%) and from 0.581 to 0.902 (55.3%), respectively, compared to ANFIS-FCM-PSOGSA1 model in the testing phase. Variation of SSL and Q with time as input positively impacted the performance of ANFIS-FCM-PSOGSA models. The

Table 5
Results of the ANFIS-FCM-PSO in modeling suspended sediment load.

Input	Cluster number	Training			R^2	Test			R^2
		RMSE	MAE	NSE		RMSE	MAE	NSE	
ANFIS-FCM-PSO1	2	6,440	2,422	0.636	0.636	4,265	1,974	0.207	0.567
ANFIS-FCM-PSO2	3	6,617	2,528	0.616	0.616	4,524	2,128	0.108	0.553
ANFIS-FCM-PSO3	2	6,263	2,849	0.656	0.661	4,353	2,364	0.174	0.548
ANFIS-FCM-PSO4	2	5,862	2,250	0.698	0.699	4,351	2,192	0.175	0.543
ANFIS-FCM-PSO5	2	3,628	1,140	0.884	0.884	1,731	687	0.869	0.874
ANFIS-FCM-PSO6	3	3,252	979	0.907	0.907	1,588	685	0.890	0.898
ANFIS-FCM-PSO7	5	3,215	972	0.909	0.909	1,576	649	0.892	0.900
ANFIS-FCM-PSO8	4	2,885	863	0.927	0.927	1,557	627	0.894	0.902
ANFIS-FCM-PSO9	5	4,134	1,125	0.850	0.861	1,556	666	0.894	0.900
ANFIS-FCM-PSO10	5	4,338	1,126	0.835	0.859	1,606	759	0.888	0.896

Note: RMSE and MAE are in t/d.

Table 6
Results of the ANFIS-FCM-PSOGSA in modeling suspended sediment load.

Model	Cluster number	Training			R^2	Test			R^2
		RMSE	MAE	NSE		RMSE	MAE	NSE	
ANFIS-FCM-PSOGSA1	10	6,324	2,437	0.649	0.649	4,107	1,925	0.265	0.581
ANFIS-FCM-PSOGSA2	5	5,920	2,371	0.692	0.692	4,184	1,946	0.237	0.574
ANFIS-FCM-PSOGSA3	10	5,755	2,371	0.709	0.709	4,262	2,017	0.208	0.563
ANFIS-FCM-PSOGSA4	5	6,068	2,542	0.677	0.677	4,323	1,992	0.185	0.555
ANFIS-FCM-PSOGSA5	3	3,651	1,162	0.883	0.883	1,678	662	0.877	0.881
ANFIS-FCM-PSOGSA6	3	3,237	1,058	0.908	0.908	1,578	629	0.892	0.900
ANFIS-FCM-PSOGSA7	5	3,245	1,011	0.908	0.908	1,554	628	0.895	0.902
ANFIS-FCM-PSOGSA8	5	2,827	930	0.930	0.930	1,520	611	0.899	0.904
ANFIS-FCM-PSOGSA9	5	3,176	1,048	0.911	0.911	1,541	658	0.896	0.903
ANFIS-FCM-PSOGSA10	3	2,845	983	0.929	0.929	1,602	750	0.888	0.895

Note: RMSE and MAE are in t/d.

ANFIS-FCM-PSOGSA8 to ANFIS-FCM-PSOGSA10 models showed a mean RMSE of 1554 t/d, MAE of 673 t/d, NSE of 0.894, and R^2 of 0.901 in the testing phase. ANFIS-FCM-PSOGSA8 improved the estimation accuracy of ANFIS-FCM-PSOGSA7 model by 2.18%, 2.71%, 0.446%, and 0.22% in terms of RMSE, MAE, NSE, and R^2, respectively.

The comparison of the performance of the best optimal models developed using the three soft computing algorithms is listed in Table 7. The ANFIS-FCM-PSOGSA8 and ANFIS-FCM-PSO8 were considered the best hybrid models based on their performances listed in Tables 5 and 6, whereas ANFIS-FCM7 was considered as the best standalone model as the variation of inputs with time showed no effect on estimation accuracy for the ANFIS-FCM based models. The ANFIS based methods also were compared with the standard sediment rating curve (SRC) model. The obtained SRC expression is

$$SSL = 0.000003Q^{2.0504} \quad (20)$$

Table 7 indicates that the SRC model provides inferior results compared to ANFIS based models with higher RMSE (4,172 t/d), MAE (1,705 t/d), and lower R^2 (0.495) and NSE (0.241) in the testing phase. Among the ANFIS based models, the standalone optimal ANFIS-FCM model was less accurate than the optimal hybrid ANFIS-FCM-PSO and ANFIS-FCM-PSOGSA models. PSO and PSOGSA based hybrid optimal ANFIS-FCM models improved the estimation accuracy of the standalone optimal ANFIS-FCM model by 2.20%–4.52%, 13.7%–15.9%, 0.449%–1.01%, and 0.557%–0.780%, in terms of RMSE, MAE, NSE and R^2, respectively, in the testing phase. Overall the comparison of model performance for the different input combinations revealed that PSOGSA was more accurate with a mean RMSE of 2,634 t/d, MAE of 1,181 t/d, NSE of 0.624, and R^2 of 0.766. It improved the performance compared to ANFIS-FCM-PSO and ANFIS-FCM by 8.14% and 1.72%, 14.7% and 5.71%, 12.5% and 2.27%, and 25.6% and 1.86%, respectively, in terms of RMSE, MAE, NSE, and R^2 in the testing phase. Overall, the models can be graded based on their performance as ANFIS-FCM-PSOGSA > ANFIS-FCM-PSO > ANFIS-FCM. The results established that the optimization of model parameters significantly improve the estimation accuracy of ANFIS-FCM models.

Visual representations of the metrics were used to evaluate the level of agreement between the observed and modeled SSL in a more comprehensive way. For this purpose, five types of visual representation plots were prepared: (i) time series plot of simulated and observed SSL; (ii) scatterplots of the observed and estimated SSL; (iii) cumulative SSL graph; (iv) violin plots; and (v) Taylor diagram. Time-series graphs (Fig. 4) demonstrate that the simulated SSL from ANFIS-FCM-PSOGSA was much closer to the observed SSL than that from the ANFIS-FCM-PSO, standalone ANFIS-FCM, and SRC models in the testing phase.

Scatter plots (Fig. 5) also indicate the superiority of ANFIS-FCM-PSOGSA model over the other models as the ANFIS-FCM-PSOGSA simulated SSL was found to be less scattered compared to the other models.

Fig. 6 shows that the ANFIS-FCM-PSOGSA model was superior in simulating cumulative SSL amounts in the testing phase compared to the other three models. Violin plots of all models were drawn to show the RMSE, MAE, and NSE.

The violin plots for the ANFIS-FCM-PSOGSA model showed lesser variation in RMSE, MAE, and NSE with flatter and shorter violins in comparison to longer and thinner violins for the other models in the testing phase (Fig. 7).

Fig. 8 shows that the standard deviation (SD) and correlation coefficient (CC) of the SRC, ANFIS-FCM, ANFIS-FCM-PSO, and ANFIS-FCM–PSOGSA models on a Taylor diagram. Taylor diagram also indicates the better estimation using the proposed optimized hybrid ANFIS-FCM-PSOGSA model as its estimates were closer to the observed data compared to the hybrid ANFIS-FCM-PSO, standalone ANFIS-FCM, and SRC models for the testing phase.

Precise estimation of the peak SSL is important for better management and operation of hydraulic structures, especially during a storm. Therefore, the SSL peak estimation capability of the proposed methods also was evaluated. Obtained results are presented in Table 8, which show the better capacity of the ANFIS-FCM-PSOGSA model in reconstructing the peak SSL than the ANFIS-FCM-PSO, ANFIS-FCM, and SRC models (see the absolute total of relative errors) in the testing phase. For example,

Table 7
Comparison of the ANFIS-FCM-PSOGSA, ANFIS-FCM-PSO, ANFIS-FCM, and SRC in modeling suspended sediment load.

Method	Input	Cluster number	Training				Test			
			RMSE	MAE	NSE	R^2	RMSE	MAE	NSE	R^2
ANFIS-FCM-PSOGSA	Q_t, Q_t–Q_{t-1}, S_{t-1}, S_{t-2}, S_{t-3}	5	2,827	930	0.930	0.930	1,520	611	0.899	0.904
ANFIS-FCM-PSO	Q_t, Q_t–Q_{t-1}, S_{t-1}, S_{t-2}, S_{t-3}	4	2,885	863	0.927	0.927	1,557	627	0.894	0.902
ANFIS-FCM	Q_t, S_{t-1}, S_{t-2} and S_{t-3}	2	3,241	1,084	0.908	0.908	1,592	727	0.890	0.897
SRC	Q_t	—	6,973	2,453	0.573	0.578	4,172	1,705	0.241	0.495

Note: RMSE and MAE are in t/d.

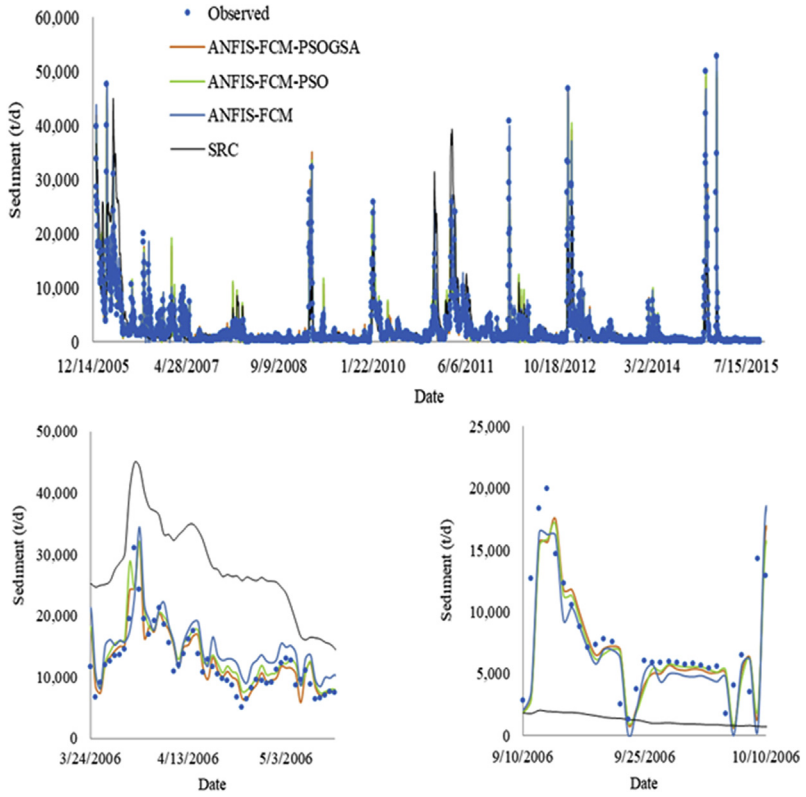

Fig. 4. Time-series plot of the observed and estimated sediment loads using the ANFIS-FCM-PSOGSA, ANFIS-FCM-PSO, ANFIS-FCM, and SRC models in the testing phase (two graphs in the bottom illustrates the two periods from the overall graph in detail).

the observed peak sediment load of 52,900 t/d was estimated by the ANFIS-PSOGSA as 38,189 t/d or underestimated by 28%. In contrast, ANFIS-FCM-PSO, ANFIS-FCM, and SRC estimated the peak sediment load as 35,805, 32,796, and 5,762 t/d or underestimated by 32%, 38%, and 89%, respectively. The ANFIS-FCM-PSOGSA model showed an absolute total error of 333, indicating a higher performance in estimating peak SSL than the ANFIS-FCM-PSO (356), ANFIS-FCM (463), and SRC (1,045) models.

4. Discussion

The PSO and PSOGSA based hybrid optimal ANFIS-FCM models enhanced the estimation skill of standalone optimal ANFIS-FCM model by 2.20%–4.52%, 13.7%–15.9%, 0.449%–1.01%, and 0.557%–0.780%, in terms of RMSE, MAE, NSE and R^2, respectively in the testing phase. Overall the comparison of model performance for different input combinations revealed that PSOGSA produced more accuracy with a mean RMSE of 2,634 t/d, MAE of 1,181 t/d, NSE of 0.624, and R^2 of 0.766, and improved the performance compared to ANFIS-FCM-PSO and ANFIS-FCM by 8.14% and 1.72%, 14.7% and 5.71%, 12.5% and 2.27%, and 25.6% and 1.86%, respectively, for the RMSE, MAE, NSE, and R^2 in the testing phase. Overall, the models' rank, based on the results, ANFIS-FCM-PSOGSA > ANFIS-FCM-PSO > ANFIS-FCM. The comparison outcomes show the importance of optimizing model parameters to significantly improve the estimation accuracy of ANFIS-FCM models. Recent studies in the literature also have found the higher skills of hybrid models compared to standalone models in SSL estimation. The fact is that hybrid models aid in finding the optimal results by reducing the drawbacks of standalone soft computing models (Kargar et al., 2021; Meshram et al., 2021; Mohammadi et al., 2021; Panahi et al., 2021; Safari, 2020).

Recent literature also showed the effectiveness of the proposed PSOGSA algorithm in finding better optimal values of model parameters, and, thus, improvement of model estimation accuracy in comparison to other optimization algorithms (Liu & Chen, 2020; Safari et al., 2020; Xu & Liu, 2020; Zhu et al., 2018). For a robust and generalized optimization algorithm, it is expected that the algorithm would able to search the best parameter for a machine learning model. The classical PSO often fails to find these parameters appropriately. Therefore, GSA algorithm is used in the current study with PSO considering their better exploitation ability. Current study also found the effectiveness of PSOGSA based ANFIS-FCM models by improving exploration and exploitation capabilities. The proposed hybrid optimization structure called PSOGSA has proved to be more effective than other optimization algorithms.

The graphical presentation revealed that all the methods overpredicted the SSL values. This can be explained by the different ranges of the training (0.02–49,770 t/d) and testing (0.055–15,390 t/d) SSL data. The models calibrated with high SSL data in the training phase tend to overpredict lower SSL data in the testing phase. This is the main disadvantage of the data-driven (DD) approaches for simulation. The other main disadvantage of the data-driven approaches is that they cannot consider the possible changes in the basin's physical and/or morphological characteristics in the modeling process. Extending the developed models to other watersheds is limited

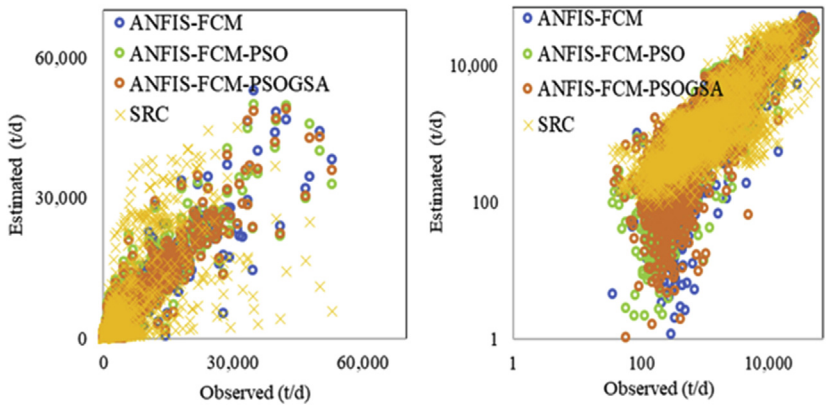

Fig. 5. Scatterplots of the observed and estimated sediment loads using the ANFIS-FCM-PSOGSA, ANFIS-FCM-PSO, ANFIS-FCM, and SRC models in the testing phase.

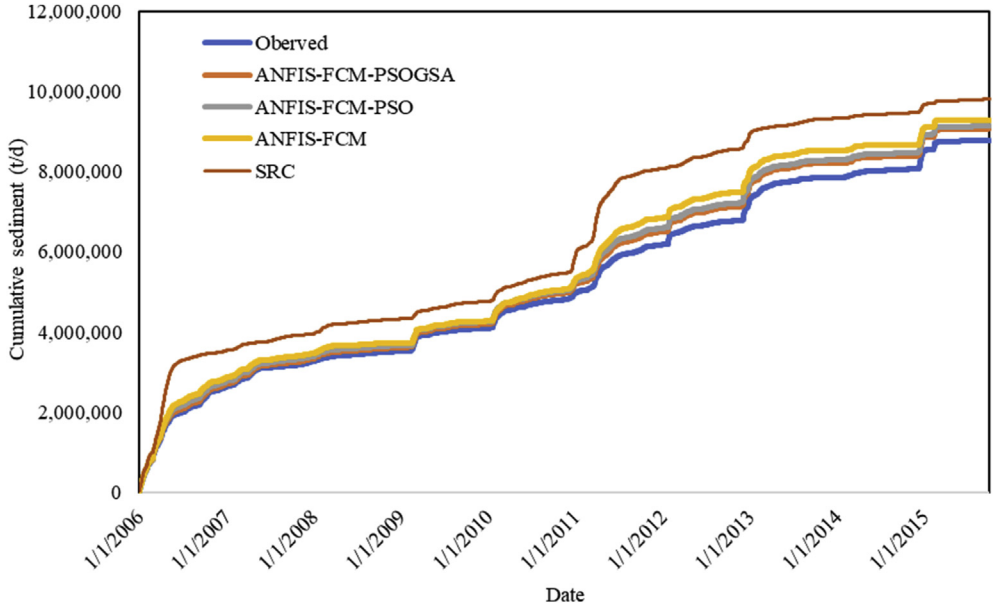

Fig. 6. Cumulative sediment loads estimated using the ANFIS-FCM-PSOGSA, ANFIS-FCM-PSO, ANFIS-FCM, and SRC models in the testing phase.

because they should be carefully calibrated with new data with a sufficient sample size. One important limitation of the current study is that the developed models use previous sediment data in estimating SSL. In the case of missing or unavailable sediment data (especially in developing countries), such models cannot be applied to estimate future SSL values. Measuring SSL is a very difficult task, and in developing countries, sufficient sediment data are not available because of technical reasons. For future research, the input parameters of the predictive models can be determined using some statistical techniques such as Gama-Test (Dehghani et al., 2019; Seifi & Riahi, 2020).

5. Conclusions

The current study investigated the capability of a new hybrid algorithm known as ANFIS-FCM-PSOGSA in modeling daily suspended sediment load. The skill of the new method was compared to the ANFIS-FCM-PSO, ANFIS-FCM, and conventional sediment rating curve methods for various input combinations, including lagged river flow and sediment values. Variation of river flow and suspended sediment with time also was considered as input to improve estimation accuracy. The current study found the following conclusions:

1) Based on the investigated river, flow discharge, Q, at time t, or the concurrent river flow significantly influenced SSL estimation.
2) Compared to Q-based inputs, antecedent SSL values (S_{t-1} to S_{t-3}) significantly influenced SSL estimation.
3) Inclusion of river flow and SSL variations with time as inputs improved the estimation capability of ANFIS-FCM-PSOGSA and ANFIS-FCM-PSO models. The improvement for ANFIS-FCM-PSOGSA was by 2.18%, 2.71%, 0.446%, and 0.22% in terms of RMSE, MAE, NSE, and R^2, respectively. The accuracy of ANFIS-FCM-PSOGSA model was superior to that of the ANFIS-FCM and ANFIS-FCM-PSO models. It improved the RMSE, MAE, NSE, and R^2 of ANFIS-FCM by 8.14%, 14.7%, 12.5%, and 25.6%, respectively.

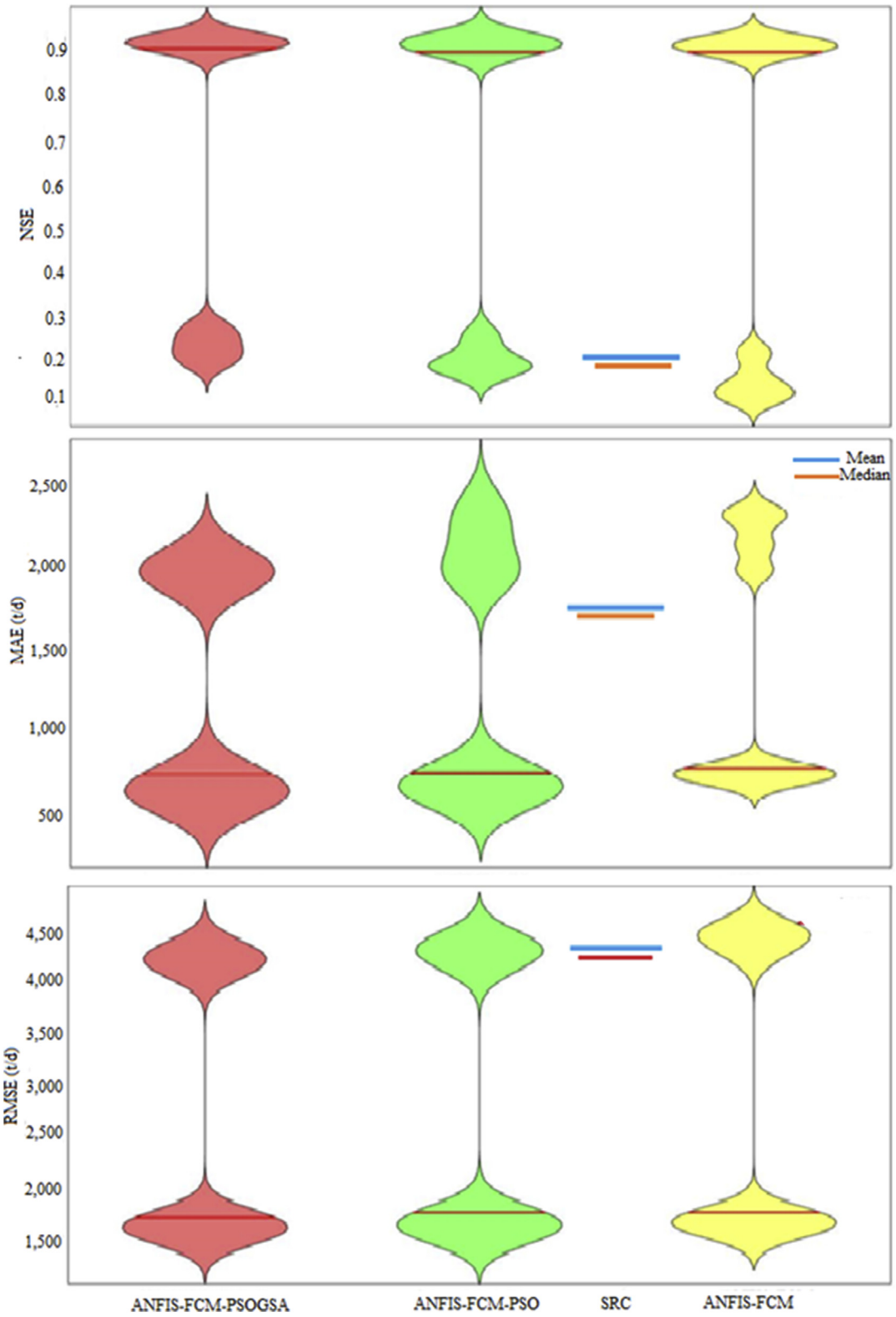

Fig. 7. Violin plots of the models showing their performance in terms of three statistical indices, NSE, MAE, and RMSE.

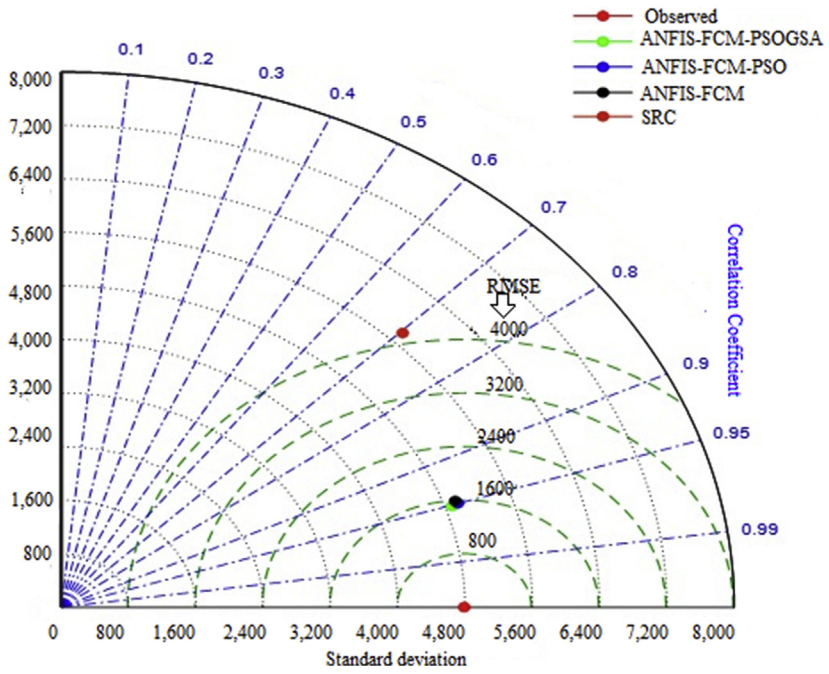

Fig. 8. Taylor diagrams of the models in simulating sediment load during the testing phase.

Table 8
Comparison of the ANFIS-FCM-PSOGSA, ANFIS-FCM-PSO, ANFIS-FCM, and SRC models in estimating peak sediment load during the testing period of the models.

Peaks >30,000 t/d	ANFIS-FCM-PSOGSA (t/d)	ANFIS-FCM-PSO (t/d)	ANFIS-FCM (t/d)	SRC (t/d)	Relative Error			
					ANFIS-FCM-PSOGSA (%)	ANFIS-FCM-PSO (%)	ANFIS-FCM (%)	SRC (%)
39,800	41,933	40,613	43,826	36,667	5	2	10	8
33,900	36,665	35,546	35,835	35,768	8	5	6	6
31,500	32,775	34,175	21,915	16,987	4	8	30	46
47,700	45,802	42,766	34,420	24,747	4	10	28	48
40,000	46,319	46,988	48,189	25,417	16	17	20	36
31,000	24,471	24,410	23,334	44,971	21	21	25	45
32,200	31,427	28,816	21,705	10,283	2	11	33	68
40,900	22,340	21,960	23,942	4057	45	46	41	90
35,700	36,162	35,205	39,948	2947	1	1	12	92
33,500	28,586	28,512	29,354	17,355	15	15	12	48
46,800	30,348	29,891	31,943	16,623	35	36	32	64
33,300	46,374	44,753	46,197	16,684	39	34	39	50
34,500	23,593	23,549	14,485	9006	32	32	58	74
50,100	43,077	40,091	44,092	11,003	14	20	12	78
42,300	48,978	49,649	46,701	14,356	16	17	10	66
33,000	35,954	34,816	34,761	15,150	9	6	5	54
52,900	38,189	35,805	32,796	5762	28	32	38	89
34,800	48,476	49,790	52,759	6227	39	43	52	82
Total (Absolute)=					333	356	463	1,045

4) Comparison of the ability of the models in simulating cumulative SSL amounts also revealed the superiority of the ANFIS-FCM-PSOGSA model compared to the SRC, ANFIS-FCM, and ANFIS-FCM-PSO models.
5) The proposed ANFIS-FCM-PSOGSA model provided a robust and reliable tool that can be applied for SSL quantification with a high degree of accuracy.

Declaration of competing interest

The authors declare that they have no known competing financial interests or personal relationships that could have appeared to influence the work reported in this paper.

References

Adedeji, P. A., Akinlabi, S. A., Madushele, N., & Olatunji, O. O. (2020). Neuro-fuzzy resource forecast in site suitability assessment for wind and solar energy: A mini review. *Journal of Cleaner Production, 269*, 122104.
Adıgüzel, E., Özer, E., Akgündoğdu, A., & Yılmaz, A. E. (2019). Prediction of dust particle size effect on efficiency of photovoltaic modules with ANFIS: An experimental study in Aegean region, Turkey. *Solar Energy, 177*, 690–702.
Adnan, R. M., Khosravinia, P., Karimi, B., & Kisi, O. (2021b). Prediction of hydraulics performance in drain envelopes using Kmeans based multivariate adaptive regression spline. *Applied Soft Computing, 100*, 107008.
Adnan, R. M., Liang, Z., El-Shafie, A., Zounemat-Kermani, M., & Kisi, O. (2019). Prediction of suspended sediment load using data-driven models. *Water, 11*(10), 2060.
Adnan, R. M., Petroselli, A., Heddam, S., Santos, C. A. G., & Kisi, O. (2021a). Short term rainfall-runoff modelling using several machine learning methods and a

conceptual event-based model. *Stochastic Environmental Research and Risk Assessment, 35*(3), 597–616.
Alizamir, M., Kisi, O., Muhammad Adnan, R., & Kuriqi, A. (2020). Modelling reference evapotranspiration by combining neuro-fuzzy and evolutionary strategies. *Acta Geophysica, 68*, 1113–1126.
Anemangely, M., Ramezanzadeh, A., & Tokhmechi, B. (2017). Shear wave travel time estimation from petrophysical logs using ANFIS-PSO algorithm: A case study from Ab-Teymour oilfield. *Journal of Natural Gas Science and Engineering, 38*, 373–387.
Aytek, A., & Kişi, Ö. (2008). A genetic programming approach to suspended sediment modelling. *Journal of Hydrology, 351*, 288–298.
Banadkooki, F. B., Ehteram, M., Ahmed, A. N., Teo, F. Y., Ebrahimi, M., Fai, C. M., … El-Shafie, A. (2020). Suspended sediment load prediction using artificial neural network and ant lion optimization algorithm. *Environmental Science and Pollution Research, 27*(30), 38094–38116.
Bounar, N., Labdai, S., & Boulkroune, A. (2019). PSO–GSA based fuzzy sliding mode controller for DFIG-based wind turbine. *ISA Transactions, 85*, 177–188.
Buyukyildiz, M., & Kumcu, S. Y. (2017). An estimation of the suspended sediment load using adaptive network based fuzzy inference system, support vector machine and artificial neural network models. *Water Resources Management, 31*(4), 1343–1359.
Calsamiglia, A., Fortesa, J., García-Comendador, J., Lucas-Borja, M. E., Calvo-Cases, A., & Estrany, J. (2018). Spatial patterns of sediment connectivity in terraced lands: Anthropogenic controls of catchment sensitivity. *Land Degradation & Development, 29*(4), 1198–1210.
Cao, Z., & Carling, P. A. (2003). On evolution of bed material waves in alluvial rivers. *Earth Surface Processes and Landforms, 28*(4), 437–441.
Chang, Q., Zhang, C., Zhang, S., & Li, B. (2019). Streamflow and sediment declines in a loess hill and gully landform basin due to climate variability and anthropogenic activities. *Water, 11*(11), 2352.
Choubin, B., Darabi, H., Rahmati, O., Sajedi-Hosseini, F., & Kløve, B. (2018a). River suspended sediment modelling using the CART model: A comparative study of machine learning techniques. *The Science of the Total Environment, 615*, 272–281.
Choubin, B., Zehtabian, G., Azareh, A., Rafiei-Sardooi, E., Sajedi-Hosseini, F., & Kişi, Ö. (2018b). Precipitation forecasting using classification and regression trees (CART) model: A comparative study of different approaches. *Environmental earth sciences, 77*(8), 1–13.
Dehghani, M., Seifi, A., & Riahi-Madvar, H. (2019). Novel forecasting models for immediate-short-term to long-term influent flow prediction by combining ANFIS and grey wolf optimization. *Journal of Hydrology, 576*, 698–725.
Dokeroglu, T., Sevinc, E., Kucukyilmaz, T., & Cosar, A. (2019). A survey on new generation metaheuristic algorithms. *Computers & Industrial Engineering, 137*, 106040.
Eappen, G., & Shankar, T. (2020). Hybrid PSO-GSA for energy efficient spectrum sensing in cognitive radio network. *Physical Communication, 40*, 101091.
Eberhart, R., & Kennedy, J. (1995). A new optimizer using particle swarm theory. In *MHS'95. Proceedings of the sixth international symposium on micro machine and human science ,october 4-6, 1995, Nageya , Japan*.
Ebtehaj, I., Bonakdari, H., Safari, M. J. S., Gharabaghi, B., Zaji, A. H., Madavar, H. R., & Mehr, A. D. (2020). Combination of sensitivity and uncertainty analyses for sediment transport modeling in sewer pipes. *International Journal of Sediment Research, 35*(2), 157–170.
Ehteram, M., Ghotbi, S., Kisi, O., Najah Ahmed, A., Hayder, G., Ming Fai, C., & El-Shafie, A. (2019). Investigation on the potential to integrate different artificial intelligence models with metaheuristic algorithms for improving river suspended sediment predictions. *Applied Sciences, 9*(19), 4149.
Emamgholizadeh, S., & Demneh, R. K. (2019). A comparison of artificial intelligence models for the estimation of daily suspended sediment load: A case study on the Telar and Kasilian rivers in Iran. *Water Supply, 19*(1), 165–178.
Enayatollahi, H., Fussey, P., & Nguyen, B. K. (2020). Modelling evaporator in organic Rankine cycle using hybrid GD-LSE ANFIS and PSO ANFIS techniques. *Thermal Science and Engineering Progress, 19*, 100570.
Faris, H., Mafarja, M. M., Heidari, A. A., Aljarah, I., Ala'M, A. Z., Mirjalili, S., & Fujita, H. (2018). An efficient binary salp swarm algorithm with crossover scheme for feature selection problems. *Knowledge-Based Systems, 154*, 43–67.
Fu, T. C. (2011). A review on time series data mining. *Engineering Applications of Artificial Intelligence, 24*(1), 164–181.
Goyal, M. K., & Ojha, C. S. P. (2011). Estimation of scour downstream of a ski-jump bucket using support vector and M5 model tree. *Water Resources Management, 25*(9), 2177–2195.
Gupta, D., Hazarika, B. B., Berlin, M., Sharma, U. M., & Mishra, K. (2021). Artificial intelligence for suspended sediment load prediction: A review. *Environmental Earth Sciences, 80*(9), 1–39.
Hebert, D., Anderson, B., Olinsky, A., & Hardin, J. M. (2014). Time series data mining: A retail application. *International journal of business analytics (IJBAN), 1*(4), 51–68.
Himanshu, S. K., Pandey, A., & Yadav, B. (2017). Assessing the applicability of TMPA-3B42V7 precipitation dataset in wavelet-support vector machine approach for suspended sediment load prediction. *Journal of Hydrology, 550*, 103–117.
Hoang, N. D., & Bui, D. T. (2018). Spatial prediction of rainfall-induced shallow landslides using gene expression programming integrated with GIS: A case study in Vietnam. *Natural Hazards, 92*(3), 1871–1887.
Hou, M., Zhang, T., Weng, F., Ali, M., Al-Ansari, N., & Yaseen, Z. M. (2018). Global solar radiation prediction using hybrid online sequential extreme learning machine model. *Energies, 11*(12), 3415.
Jang, J. S. (1993). ANFIS: Adaptive-network-based fuzzy inference system. *IEEE transactions on systems, man, and cybernetics, 23*(3), 665–685.
Jiang, S., Ji, Z., & Shen, Y. (2014). A novel hybrid particle swarm optimization and gravitational search algorithm for solving economic emission load dispatch problems with various practical constraints. *International Journal of Electrical Power & Energy Systems, 55*, 628–644.
Jiang, J., Yang, X., Meng, X., & Li, K. (2020). Enhance chaotic gravitational search algorithm (CGSA) by balance adjustment mechanism and sine randomness function for continuous optimization problems. *Physica A: Statistical Mechanics and Its Applications, 537*, 122621.
Kargar, K., Safari, M. J. S., & Khosravi, K. (2021). Weighted instances handler wrapper and rotation forest-based hybrid algorithms for sediment transport modeling. *Journal of Hydrology, 598*, 126452.
Kaur, H., Alam, M. A., Mariyam, S., Alankar, B., Chauhan, R., Adnan, R. M., & Kisi, O. (2021). Predicting water availability in water bodies under the influence of precipitation and water management Actions using VAR/VECM/LSTM. *Climate, 9*(9), 144.
Khan, M. Y. A., Hasan, F., & Tian, F. (2019). Estimation of suspended sediment load using three neural network algorithms in Ramganga River catchment of Ganga Basin, India. *Sustainable Water Resources Management, 5*(3), 1115–1131.
Khosravi, K., Daggupati, P., Alami, M. T., Awadh, S. M., Ghareb, M. I., Panahi, M.,., & Yaseen, Z. M. (2019). Meteorological data mining and hybrid data-intelligence models for reference evaporation simulation: A case study in Iraq. *Computers and Electronics in Agriculture, 167*, 105041.
Khosravi, K., Mao, L., Kisi, O., Yaseen, Z. M., & Shahid, S. (2018). Quantifying hourly suspended sediment load using data mining models: Case study of a glacierized andean catchment in Chile. *Journal of Hydrology, 567*, 165–179.
Kisi, O., Shiri, J., Karimi, S., & Adnan, R. M. (2018). Three different adaptive neuro fuzzy computing techniques for forecasting long-period daily streamflows. In *Big data in engineering applications* (pp. 303–321). Singapore: Springer.
Kleist, C. (2015). *Time series data mining methods* (Master dissertation). Humboldt-Universität zu Berlin, Germany.
Lafdani, E. K., Nia, A. M., & Ahmadi, A. (2013). Daily suspended sediment load prediction using artificial neural networks and support vector machines. *Journal of Hydrology, 478*, 50–62.
Liu, H., & Chen, C. (2020). Prediction of outdoor PM2.5 concentrations based on a three-stage hybrid neural network model. *Atmospheric Pollution Research, 11*(3), 469–481.
Mallick, S., Ghoshal, S. P., Acharjee, P., & Thakur, S. S. (2013). Optimal static state estimation using improved particle swarm optimization and gravitational search algorithm. *International Journal of Electrical Power & Energy Systems, 52*, 254–265.
Meshram, S. G., Ghorbani, M. A., Deo, R. C., Kashani, M. H., Meshram, C., & Karimi, V. (2019a). New approach for sediment yield forecasting with a two-phase feed-forward neuron network-particle swarm optimization model integrated with the gravitational search algorithm. *Water Resources Management, 33*(7), 2335–2356.
Meshram, S. G., Ghorbani, M. A., Shamshirband, S., Karimi, V., & Meshram, C. (2019b). River flow prediction using hybrid PSOGSA algorithm based on feed-forward neural network. *Soft Computing, 23*(20), 10429–10438.
Meshram, S. G., Safari, M. J. S., Khosravi, K., & Meshram, C. (2021). Iterative classifier optimizer-based pace regression and random forest hybrid models for suspended sediment load prediction. *Environmental Science and Pollution Research, 28*(9), 11637–11649.
Mirjalili, S., Hashim, S. Z. M., & Sardroudi, H. M. (2012). Training feedforward neural networks using hybrid particle swarm optimization and gravitational search algorithm. *Applied Mathematics and Computation, 218*(22), 11125–11137.
Misset, C., Recking, A., Navratil, O., Legout, C., Poirel, A., Cazilhac, M., … Esteves, M. (2019). Quantifying bed-related suspended load in gravel bed rivers through an analysis of the bedload-suspended load relationship. *Earth Surface Processes and Landforms, 44*(9), 1722–1733.
Mohammadian, A., Tajrishi, M., & Azad, F. L. (2004). Two dimensional numerical simulation of flow and geo-morphological processes near headlands by using unstructured grid. *International Journal of Sediment Research, 19*(4), 258–277.
Mohammadi, B., Guan, Y., Moazenzadeh, R., & Safari, M. J. S. (2021). Implementation of hybrid particle swarm optimization-differential evolution algorithms coupled with multi-layer perceptron for suspended sediment load estimation. *Catena, 198*, 105024.
Mosa, M. A. (2020). A novel hybrid particle swarm optimization and gravitational search algorithm for multi-objective optimization of text mining. *Applied Soft Computing, 90*, 106189.
Muhammad Adnan, R., Yuan, X., Kisi, O., Yuan, Y., Tayyab, M., & Lei, X. (2019). Application of soft computing models in streamflow forecasting. *Proceedings of the institution of civil engineers-water management, 172*(3), 123–134.
Naderpour, H., & Mirrashid, M. (2020). Estimating the compressive strength of eco-friendly concrete incorporating recycled coarse aggregate using neuro-fuzzy approach. *Journal of Cleaner Production, 265*, 121886. Naderpour, H., & Mirrashid, M. (2020).
Naganna, S. R., Deka, P. C., Ghorbani, M. A., Biazar, S. M., Al-Ansari, N., & Yaseen, Z. M. (2019). Dew point temperature estimation: Application of artificial intelligence model integrated with nature-inspired optimization algorithms. *Water, 11*(4), 742.

Nourani, V., & Andalib, G. (2015). Daily and monthly suspended sediment load predictions using wavelet based artificial intelligence approaches. *Journal of Mountain Science, 12*(1), 85–100.

Olyaie, E., Banejad, H., Chau, K. W., & Melesse, A. M. (2015). A comparison of various artificial intelligence approaches performance for estimating suspended sediment load of river systems: A case study in United States. *Environmental Monitoring and Assessment, 187*(4), 1–22.

Özger, M., & Kabataş, M. B. (2015). Sediment load prediction by combined fuzzy logic-wavelet method. *Journal of Hydroinformatics, 17*(6), 930–942.

Özkaraca, O. (2018). A comparative evaluation of Gravitational Search Algorithm (GSA) against Artificial Bee Colony (ABC) for thermodynamic performance of a geothermal power plant. *Energy, 165*, 1061–1077.

Panahi, F., Ehteram, M., & Emami, M. (2021). Suspended sediment load prediction based on soft computing models and Black Widow Optimization Algorithm using an enhanced gamma test. *Environmental Science and Pollution Research, 28*, 48253–48273.

Rajaee, T., & Jafari, H. (2020). Two decades on the artificial intelligence models advancement for modeling river sediment concentration: State-of-the-art. *Journal of Hydrology, 588*, 125011.

Rashedi, E., Rashedi, E., & Nezamabadi-pour, H. (2018). A comprehensive survey on gravitational search algorithm. *Swarm and evolutionary computation, 41*, 141–158.

Ray, R., Kumar, D., Samui, P., Roy, L. B., Goh, A. T. C., & Zhang, W. (2021). Application of soft computing techniques for shallow foundation reliability in geotechnical engineering. *Geoscience Frontiers, 12*(1), 375–383.

Rezaei, K., Pradhan, B., Vadiati, M., & Nadiri, A. A. (2021). Suspended sediment load prediction using artificial intelligence techniques: Comparison between four state-of-the-art artificial neural network techniques. *Arabian Journal of Geosciences, 14*(3), 1–13.

Safari, M. J. S. (2020). Hybridization of multivariate adaptive regression splines and random forest models with an empirical equation for sediment deposition prediction in open channel flow. *Journal of Hydrology, 590*, 125392.

Safari, M. J. S., Mohammadi, B., & Kargar, K. (2020). Invasive weed optimization-based adaptive neuro-fuzzy inference system hybrid model for sediment transport with a bed deposit. *Journal of Cleaner Production, 276*, 124267.

Sakurai, Y., Matsubara, Y., & Faloutsos, C. (2015). Mining and forecasting of big time-series data. In *Proceedings of the 2015 ACM SIGMOD international conference on management of data, may 31-June 04, 2015, melbourne, Australia*.

Salih, S. Q., Allawi, M. F., Yousif, A. A., Armanuos, A. M., Saggi, M. K., Ali, M., & Chau, K.-W. (2019). Viability of the advanced adaptive neuro-fuzzy inference system model on reservoir evaporation process simulation: case study of Nasser Lake in Egypt. *Engineering Applications of Computational Fluid Mechanics, 13*(1), 878–891. https://doi.org/10.1080/19942060.2019.1647879.

Salih, S. Q., Sharafati, A., Khosravi, K., Faris, H., Kisi, O., Tao, H., & Yaseen, Z. M. (2020). River suspended sediment load prediction based on river discharge information: Application of newly developed data mining models. *Hydrological Sciences Journal, 65*(4), 624–637.

Samadi, M., Jabbari, E., & Azamathulla, H. M. (2014). Assessment of M5′ model tree and classification and regression trees for prediction of scour depth below free overfall spillways. *Neural Computing & Applications, 24*(2), 357–366.

Samantaray, S., & Ghose, D. K. (2018). Evaluation of suspended sediment concentration using descent neural networks. *Procedia computer science, 132*, 1824–1831.

Seifi, A., & Riahi, H. (2020). Estimating daily reference evapotranspiration using hybrid gamma test-least square support vector machine, gamma test-ANN, and gamma test-ANFIS models in an arid area of Iran. *Journal of Water and Climate Change, 11*(1), 217–240.

Shamaei, E., & Kaedi, M. (2016). Suspended sediment concentration estimation by stacking the genetic programming and neuro-fuzzy predictions. *Applied Soft Computing, 45*, 187–196.

Sharafati, A., Haghbin, M., Aldlemy, M. S., Mussa, M. H., Al Zand, A. W., Ali, M.,., & Yaseen, Z. M. (2020a). Development of advanced computer aid model for shear strength of concrete slender beam prediction. *Applied Sciences, 10*(11), 3811.

Sharafati, A., Haji Seyed Asadollah, S. B., Motta, D., & Yaseen, Z. M. (2020b). Application of newly developed ensemble machine learning models for daily suspended sediment load prediction and related uncertainty analysis. *Hydrological Sciences Journal, 65*(12), 2022–2042.

Sharafati, A., Tafarojnoruz, A., Motta, D., & Yaseen, Z. M. (2020c). Application of nature-inspired optimization algorithms to ANFIS model to predict wave-induced scour depth around pipelines. *Journal of Hydroinformatics, 22*(6), 1425–1451.

Shiau, J. T., & Chen, T. J. (2015). Quantile regression-based probabilistic estimation scheme for daily and annual suspended sediment loads. *Water Resources Management, 29*(8), 2805–2818.

Soroush, E., Mesbah, M., Hajilary, N., & Rezakazemi, M. (2019). ANFIS modeling for prediction of CO_2 solubility in potassium and sodium based amino acid Salt solutions. *Journal of Environmental Chemical Engineering, 7*(1), 102925.

Talebi, A., Mahjoobi, J., Dastorani, M. T., & Moosavi, V. (2017). Estimation of suspended sediment load using regression trees and model trees approaches (Case study: Hyderabad drainage basin in Iran). *ISH Journal of Hydraulic Engineering, 23*(2), 212–219.

Tao, H., Keshtegar, B., & Yaseen, Z. M. (2019). The feasibility of integrative radial basis M5Tree predictive model for river suspended sediment load simulation. *Water Resources Management, 33*(13), 4471–4490.

Tayfur, G., Karimi, Y., & Singh, V. P. (2013). Principle component analysis in conjuction with data driven methods for sediment load prediction. *Water Resources Management, 27*(7), 2541–2554.

Xu, Y., & Liu, H. (2020). Spatial ensemble prediction of hourly PM2. 5 concentrations around Beijing railway station in China. *Air Quality, Atmosphere & Health, 13*(5), 563–573.

Yuan, X., Chen, C., Lei, X., Yuan, Y., & Adnan, R. M. (2018). Monthly runoff forecasting based on LSTM–ALO model. *Stochastic Environmental Research and Risk Assessment, 32*(8), 2199–2212.

Zanganeh, M. (2020). Improvement of the ANFIS-based wave predictor models by the particle swarm optimization. *Journal of Ocean Engineering and Science, 5*, 84–99.

Zare, M., & Koch, M. (2018). Groundwater level fluctuations simulation and prediction by ANFIS-and hybrid Wavelet-ANFIS/Fuzzy C-Means (FCM) clustering models: Application to the Miandarband plain. *Journal of Hydro-environment Research, 18*, 63–76.

Zhu, S., Lian, X., Wei, L., Che, J., Shen, X., Yang, L., & Li, J. (2018). PM2. 5 forecasting using SVR with PSOGSA algorithm based on CEEMD, GRNN and GCA considering meteorological factors. *Atmospheric environment, 183*, 20–32.

Zounemat-Kermani, M., Mahdavi-Meymand, A., Alizamir, M., Adarsh, S., & Yaseen, Z. M. (2020a). On the complexities of sediment load modeling using integrative machine learning: Application of the great river of Loíza in Puerto Rico. *Journal of Hydrology, 585*, 124759.

Zounemat-Kermani, M., Matta, E., Cominola, A., Xia, X., Zhang, Q., Liang, Q., & Hinkelmann, R. (2020b). Neurocomputing in surface water hydrology and hydraulics: A review of two decades retrospective, current status and future prospects. *Journal of Hydrology, 588*, 125085.